

Comparative molecular docking studies of EGCG with SHaPrP^C

Abstract

Epigallocatechin gallate (EGCG) is a naturally occurring alkaloid found in green tea. It has been shown to bind with nanomolar affinity to the monomeric prion protein and induce conformational instability. A better understanding of the specific molecular interactions that impart this strong interaction and molecular rearrangement are of interest for the development of ligands that possess both high affinity yet impart stabilizing effects. Recently, it has been demonstrated that molecules with such characteristics reduce PrP^{Sc} titers in both *in-vitro* and *ex-vivo* experiments. To gain structural insights into EGCG's effect on the monomeric prion protein (PrP^C), comparative molecular docking studies of EGCG was performed against SHaPrP^C using MOE, Sybyl and FlexX software docking programs. These results show that the side orientations of Tyr¹⁶⁹ and Tyr²¹⁸ play an important role in binding of EGCG near the amyloyme region motif between loop-2 and helix-2.

Keywords: docking, EGCG, SHaPrP^C

Volume 2 Issue 5 - 2018

Nataraj Sekhar Pagadala,¹ Rolando Perez-Pineiro,² Trent C Bjorn Dahl,² David S Wishart²

¹Department of Medical Microbiology and Immunology, University of Alberta, Canada

²Departments of Biological Sciences, and Computing Science, University of Alberta, Canada

Correspondence: Nataraj Sekhar Pagadala, Department of Medical Microbiology and Immunology, University of Alberta, Canada, Email nattu251@gmail.com

Received: July 29, 2018 | **Published:** September 24, 2018

Introduction

The infectious prions can act as self-replicating agents.¹ The disease progresses by conformational transition, utilizing cellular PrP (PrP^C) as substrate.² This transforms endogenous α -helix-rich PrP^C to β -sheet-rich, disease-causing proteolytic resistant conformations (PrP^{Sc}).³⁻⁷ However, recently it has been shown that PrP^{Sc} forms amyloid fibrils some of which are protease sensitive.⁸⁻¹³ *In vitro* experiment on recombinantly expressed and refolded PrP (rPrP) show that EGCG (epigallocatechin-3-gallate) promotes the formation of random coil structure destabilizing the natively folded rPrP. These random coil conformers formed by EGCG were initially monomeric and further converted to PK-sensitive aggregates.¹⁴ It was also shown that EGCG elicits switching the susceptible form Sup35 prions to resistant forms *In vivo*.¹⁵ In this study, we show that epigallocatechin gallate (EGCG), the major polyphenol in green tea, bind to pocket A near amyloyme region of SHaPrP^C and might induce rapid transition of PrP^C into a detergent-insoluble conformation

Methodology

MOE 2009.10 (Chemical computing group, Montreal, Canada) and SybylX 1.3 (SYBYL-X 1.3, Tripos International, 1699 South Hanley Rd., St. Louis, Missouri, 63144, USA) were used for *in-silico* docking studies. Initially, in order to identify a suitable PrP model for docking, structures from NMR ensemble of Syrian hamster PrP further referred as SHaPrP (PDB ID: 1B10) were superimposed and an average structure was calculated by MOE. Pair-wise alignment of each model from the NMR ensemble with the average structure revealed that model #17 had the smallest RMSD of 0.5Å. This model was energy minimized with CHARMM27 force field using generalized born implicit solvent representation.¹⁶ To take into account a possible role of PrP-bound water molecules in PrP-EGCG binding, water coordinates from X-ray structure of human prion protein (PDB ID: 3HAF) were transferred to the model of hamster PrP. In order to achieve this, the hamster PrP model was superimposed with the X-ray

structure of human PrP and coordinates of 26 water molecules from the X-ray structure were appended to coordinates of the superimposed hamster PrP model. MOE alpha site finder was used to identify SHaPrP binding pocket. The rotamer orientations of the residues in the binding pocket with a distance radius of 1.2Å that provided the maximal hydrophobicity of the binding pocket near the amyloyme region were predicted using rotamer explorer of MOE and were used further in docking simulations using MOE. For *In silico* docking in MOE, the ligand placement method "Alpha PMI" was employed to bias the conformational search of the ligand to meaningful trials by aligning and matching all triangles of the template points with compatible geometry using London dG scoring function. Monte Carlo method of simulated annealing was used to find the global minimum by exploring various states of a configuration space with small changes in the current state. Each new state is accepted or rejected according to Metropolis criterion. Binding poses, which were initially identified during the simulated annealing step, were further optimized by energy minimization with the Tripos Assisted Force Field for small molecules. Finally, relative binding free energies, electrostatic energy, vander Waals energy, and solvation energy were calculated (i.e., solvent electrostatic correction). Solvation energies were calculated using Poisson-Boltzmann equation. The reaction model dielectric function with a cut-off between 8 and 10Å and the pocket radius of 6.0Å was used for our docking studies. For *In silico* docking using Surflex X, an idealized active site ligand (called a protomol) is generated from the protein structure. The protomol construction is based solely on the hydrogen atoms of the protein residues that constitute the active site. The parameters used to produce small and buried target are proto_thresh=0.5 and proto_bloat=0. Ligand is docked in mol2 format using the whole molecule approach. The input ligand is fragmented into 1-10 molecular fragments with some rotatable bonds for each fragment. Each fragment is conformationally searched and a maximum of 100 conformations per fragment is generated in each stage of the incremental construction process. Each conformation of each fragment is aligned to the protomol to yield

poses that maximize molecular similarity to the protomol. Finally, the aligned fragments are scored and pruned on the basis of the scoring function and the degree of protein interpenetration. The whole protein is considered in all the two docking programs. The binding poses with high affinity that were obtained from two different docking calculations were further minimized in the binding pocket with ligX program of MOE using TAFF force field. In order to compare results from different docking program in a uniform manner, stability of PrP–EGCG complexes was tested with molecular dynamics using the CHARMM27 force field distributed in MOE, starting from the fully minimized structures in the (NVT) ensemble at a temperature of 300K. An integration time step of 0.5fs was used. No restraints were applied to atomic positions. No explicit water was added and born solvation dielectric was used. The total simulation time was 10000ps. The root-mean-square deviations (rmsd) of the ligand conformations in the binding pocket were calculated from each trajectory to quantify the stability of the protein–ligand complex.

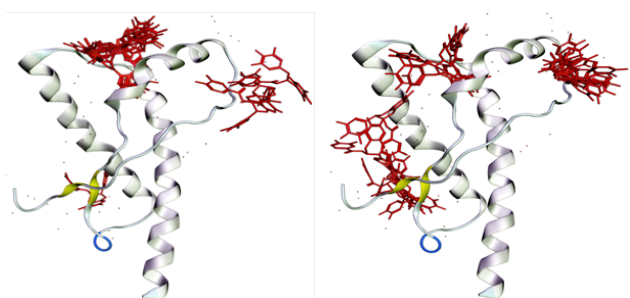
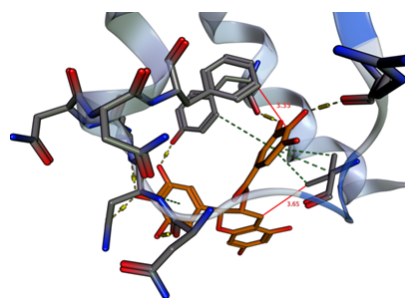
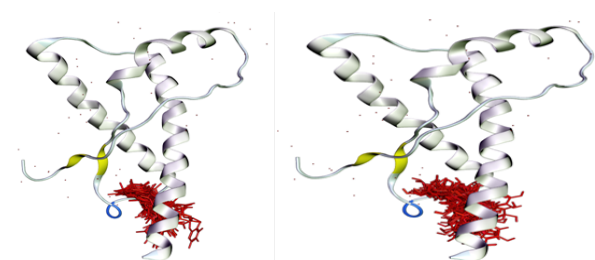
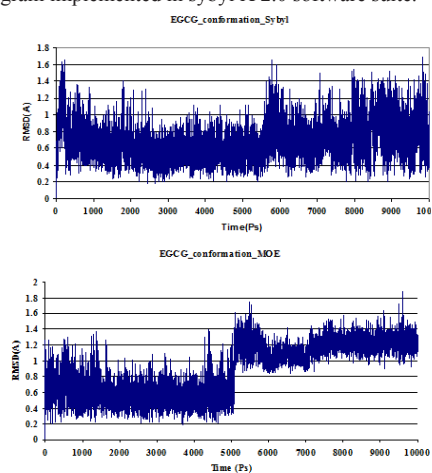
Results and discussion

Out of thirty that were used as cut-off for blind docking study using MOE, only seventeen poses were able to bind with the negative binding free energy. Out of seventeen poses, only single pose prefers to bind near amyloyme region, four poses bind near pocket the so-called thiamine binding site and the remaining twelve poses bind in the binding pocketD near Glu¹⁹⁶ where known inhibitor GN8 binds in MoSHaPrP.^{17–19} These results reveal that the largest cluster of EGCG prefer to bind GN8 pocket with the top pose binding with highest affinity of –9.3Kcal/Mol Figure 1A. Further, docking studies of EGCG was performed with the energy minimized structure of model #17 in the presence of water and ions. The side chain orientations of Tyr¹⁶⁹, Phe¹⁷⁵ and Tyr²¹⁸ containing aromatic rings that provided the maximal hydrophobicity of the binding pocket were also used in docking simulations. The RMSD of C α between the native and energy minimized structures were 1.5Å. Out of seventeen poses that bind with negative binding affinity, five poses bind to pocket A nearer amyloyme motif (NNQNNF) on the outer surface of SHaPrP^C, seven poses bind to pocket B between loop1 and α 1 near Tyr¹⁵⁰ that was identified as thiamine binding site, three poses bind to pocket D near Glu¹⁹⁶ and two poses bind to pocket C near His¹⁸⁶ Figure 1B. The top pose that prefers pocket A amyloyme region binds with high affinity of –10.2Kcal/mol. These docking results on native and energy minimized structure of SHaPrP^C (model#17) reveals that EGCG binding shifts from pocket D (GN8 pocket) to pocket B (thiamine binding site) and pocket A (amyloyme motif region). Binding pocket analysis for the energy minimized structure showed pocket A (amyloyme motif region) was top ranked (Pocket size of 90Å and number of side chain atoms of 68 including fifteen hydrophobic atoms with higher number of solvent exposed atoms) Figure 1B. In the energy minimized model, the native orientation of Tyr¹⁶⁹ side chain orients with χ^1 of 75.1° and χ^2 of 76.6° and Phe¹⁷⁵ side chain orients with χ^1 of –172.3° and χ^2 of –88.5°. Side chain analysis of Tyr¹⁶⁹ showed three rotamers with χ^1 and χ^2 of 75 and 62°, 93 and 78°, and –83 and –68° respectively. The first two rotamers doesn't show any significant increase in the number of hydrophobic atoms of the binding pocket and are not considered further. But rotamer 3 allows the side chain to orient in the opposite direction compared to native orientation and opens the new binding pocket with tight atomic packing between loop3 and helix3 near the pocket A (amyloyme region) with the residues Val¹⁶⁶, Tyr¹⁶⁹, Asn¹⁷⁰,

Asn¹⁷², Gln¹⁷², Phe¹⁷⁵, Gln²¹⁷, Tyr²¹⁸, Glu²²¹ and Ser²²² (pocket size of 64 and side chain atoms of 41 including 12 hydrophobic atoms with less number of solvent exposed residues). Blind docking of EGCG performed against SHaPrP^C with new side chain orientation for Tyr¹⁶⁹ (χ^1 of –83° and χ^2 of –68°) along with structural water and ions show all the thirty conformations occupy the new binding pocket A between loop3 and helix3 near the amyloyme region Figure 2A. The high affinity conformation with –14.6Kcal/mol show one hydrogen bonding and two hydrophobic interactions with Ser²²² (N), Val¹⁶⁶ (C γ^2) and Phe¹⁷⁵(Ce²) with O6, C7 and C15 atoms of the ligand respectively. The higher binding energy implies an important role that Tyr¹⁶⁹ of SHaPrP^C plays in binding EGCG. Rotamer optimization of Phe¹⁷⁵ did not result in improved hydrophobicity of the binding pocket. Therefore, the native orientation of Phe¹⁷⁵ side-chain was used in our docking studies. Overall, four side chain rotamers were predicted for Tyr²¹⁸. First two rotamers corresponding to experimental structure do not show any significant increase in the number of hydrophobic atoms and size of the pocket and were not considered further. The third rotamer of Tyr²¹⁸ with specific angles of χ^1 of –158° and χ^2 of 70° (pocket size with 69 and side chain atoms with 43 including 12 hydrophobic atoms) show variations in the size and hydrophobicity of the binding pocket was used for further docking studies. Blind docking of EGCG in the presence of water and ions with new side chain orientations of Tyr²¹⁸ allows to bind with a high affinity of –15.9Kcal/mol and –14.7Kcal/mol compared to optimized structure of Tyr¹⁶⁹ Figure 2B. The conformation with high affinity when further minimized in the binding pocket using lig X with new side chain orientations of Tyr¹⁶⁹ (rotamer3) and Tyr²¹⁸ (rotamer3) show six hydrogen bonding and two hydrophobic interactions with Asp¹⁶⁷, Gln¹⁷², Gln²¹⁷, Tyr²¹⁸, Ser²²², Tyr²²⁵, Val¹⁶⁶ and Phe¹⁷⁵ residues respectively Table1. In order to ensure that MOE results are not an artifact of MOE scoring function, docking was also conducted using other commonly used program, such as Surflex with the final structure of SHaPrP^C with new side chain orientations of Tyr¹⁶⁹ (rotamer3) and Tyr²¹⁸ (rotamer3). Docking studies carried out using Surflex also showed EGCG binding to the new binding pocket A between loop3 and helix3 near the amyloyme region. Analysis of the top Surflex binding pose revealed that EGCG orientation in the binding pocket is stabilized by seven hydrogen bonds and two hydrophobic interactions between EGCG and PrP^C residues Pro¹⁶⁵, Asn¹⁷¹, Gln¹⁷², Gln²¹⁷, Tyr²¹⁸, Ser²¹⁸, Ser²²², Tyr²²⁵, Val¹⁶⁶ and Phe¹⁷⁵ Table 1 and Figure 3. These docking results based on MOE and surflex X reveals that the conformation generated by surflex X show more number of interactions with the amino acids involved in Pocket A. Binding free energy in terms of ΔG calculated using Hyde module of Flex X to recalculate ΔG for top binding poses from two different programs also showed that the conformation of EGCG generated by surflex X binds with high G of –16Kj/mol. These results show that the conformation generated by surflex X is the most probable conformation and the side orientations of Tyr¹⁶⁹ and Tyr²¹⁸ play an important role in binding of EGCG to pocket A near the amyloyme region motif between loop–2 and helix–2. Stability of EGCG–SHaPrP^C complexes under a more accurate Generalized Born representation of solvation effects was studied with MOE molecular dynamics. Stability of EGCG–SHaPrP^C binding poses was evaluated by calculating RMSD of the ligand as a function of simulation time. Molecular dynamics revealed that the top binding pose of EGCG–SHaPrP^C complex generated by Surflex Figure 4A is more stable than the top binding poses produced by MOE Figure 4B.

Table 1 Ligand–protein contacts of EGCG top binding poses generated using MOE and SYBYLX 2.0 software suite near pocketA of SHaPrP^C

Software	Ligand contacts before energy minimization		Ligand contacts after energy minimization	
	Hydrogen bonding	Hydrophobic	Hydrogen bonding	Hydrophobic
MOE	Arg164.O—O7Lig	Val166.Cg1—C14	Asp167.Od1—O4Lig	Val166.Cg1—C5Lig
	Pro165.O—O4Lig	Phe175.Ce2—C21	Gln172.N—O6Lig	Phe175.Ce2—C3Lig
	Val166.O—O4Lig		Gln217.O—O3Lig	
	Tyr169.O—O6Lig		Tyr218.O—O3Lig	
	Asn170.O—O6Lig		Ser222.N—O3Lig	
			Tyr225.O—O7Lig	
Sybyl	Asn171.Od1—OLig	VAL166.CG1—CLig	PRO165.O—OLig	VAL166.CG1—CLig
	GLN172.N—OLig	PHE175.CE2—CLig	ASN171.OD1—OLig	PHE175.CE2—CLig
	TYR218.O—OLig		GLN172.N—OLig	
	SER222.N—OLig		GLN217.O—OLig	
			TYR218.O—OLig	
			SER222.N—OLig	
		TYR225.O—OLig		

**Figure 1** (A) Blind docking results of EGCG with SHaPrP^C NMR model (1B10:17), (B) for the energy–minimized structure of SHaPrP^C (1B10:17) in the presence of water and ions.**Figure 3** Ligand protein interaction of EGCG with SHaPrP^C using surflex X docking program implemented in sybyl X 2.0 software suite.**Figure 2** Blind docking of EGCG performed against SHaPrP^C with new side chain orientation for Tyr¹⁶⁹ (χ_1 of -83° and 2 of -68°) (A) Tyr²¹⁸ (B) along with structural water and ions.**Figure 4** Calculated RMSD graphs of MD simulations for the top binding poses of EGCG–SHaPrP^C generated using SybylX2.0 (A) and MOE (B) using NAMD software. Time (ps) is taken on X–axis and RMSD on Y–axis.

Conclusion

Molecular docking studies show that ECGC binds to pocket A between loop3 and helix3 of SHaPrP^C interacting with Tyr¹⁶⁹ and Tyr²¹⁸.

Acknowledgements

I thank Dr. Wishart, Department of Computing Science and Biological Sciences, university of alberta, Edmonton, Canada, for providing the laboratory facilities and helpful discussions.

Conflict of interest

Authors declare that there is no conflict of interest.

References

1. Prusiner SB. Novel proteinaceous infectious particles cause scrapie. *Science*. 1982;216(4542):136–144.
2. Prusiner SB. Shattuck lecture—neurodegenerative diseases and prions. *The New England journal of medicine*. 2001;344(20):1516–1526.
3. Pan YT, Hori H, Saul R, et al. Castanospermine inhibits the processing of the oligosaccharide portion of the influenza viral hemagglutinin. *Biochemistry*. 1983;22(16):3975–3984.
4. Basler K, Oesch B, Scott M, et al. Scrapie and cellular PrP isoforms are encoded by the same chromosomal gene. *Cell*. 1986;46(3):417–428.
5. Bolton DC, Kinley MP, Prusiner SB. Identification of a protein that purifies with the scrapie prion. *Science*. 1982;218(4579):1309–1311.
6. Prusiner SB, Kinley MP, Bowman KA, et al. Scrapie prions aggregate to form amyloid-like birefringent rods. *Cell*. 1983;35(1):349–358.
7. Meyer RK, Kinley MP, Bowman KA, et al. Separation and properties of cellular and scrapie prion proteins. *Proceedings of the National Academy of Sciences of the United States of America*. 1986;83(8):2310–2314.
8. Safar J, Wille H, Itri V, et al. Eight prion strains have PrP(Sc) molecules with different conformations. *Nature medicine*. 1998;4:1157–1165.
9. Tzaban S, Friedlander G, Schonberger O, et al. Protease-sensitive scrapie prion protein in aggregates of heterogeneous sizes. *Biochemistry*. 2002;41(42):12868–12875.
10. Tremblay P, Ball HL, Kaneko K, et al. PrP^{Sc} conformers induced by a synthetic peptide and several prion strains. *Journal of virology*. 2004;78(4):2088–2099.
11. Legname G, Nguyen HO, Peretz D, et al. Continuum of prion protein structures enciphers a multitude of prion isolate-specified phenotypes. *Proceedings of the National Academy of Sciences of the United States of America*. 2006;103(50):19105–19110.
12. Pastrana MA, Sajjani G, Onisko B, et al. Isolation and characterization of a proteinase K-sensitive PrP^{Sc} fraction. *Biochemistry*. 2006;45(51):15710–15717.
13. Colby DW, Zhang Q, Wang S, et al. Prion detection by an amyloid seeding assay. *Proceedings of the National Academy of Sciences*. 2007;104(52):20914–20919.
14. Rambold AS, Muller V, Ron U, et al. Stress-protective signaling of prion protein is corrupted by scrapie prions. *The EMBO journal*. 2008;27(14):1974–1984.
15. Roberts BE, Duennwald ML, Wang H, et al. A synergistic small-molecule combination directly eradicates diverse prion strain structures. *Nature chemical biology*. 2009;5(12):936–946.
16. Mackerell AD. Empirical force fields for biological macromolecules: overview and issues. *Journal of computational chemistry*. 2004;25(13):1584–1604.
17. Perez-Pineiro R, Bjorndahl TC, Berjanskii MV, et al. The prion protein binds thiamine. *The FEBS journal*. 2011;278(21):4002–4014.
18. Kuwata K, Nishida N, Matsumoto T, et al. Hot spots in prion protein for pathogenic conversion. *Proceedings of the National Academy of Sciences of the United States of America*. 2007;104(29):11921–11926.
19. Pagadala NS, Bjorndahl TC, Blinov N, et al. Molecular docking of thiamine reveals similarity in binding properties between the prion protein and other thiamine-binding proteins. *Journal of molecular modeling*. 2013;19(12):5225–5235.